Computer Simulations to Study Diffraction Effects of Stacking Faults in β-SiC : II. Experimental Verification

Vijay V. Pujar*† and James. D. Cawley*

Department of Materials Science and Engineering, Case School of Engineering

Case Western Reserve University, Cleveland, OH 44106-7204

Earlier results from computer simulation studies suggest a correlation between the spatial distribution of stacking errors in the β-SiC structure and features observed in X-ray diffraction patterns of the material. Reported here are experimental results obtained from two types of nominally β-SiC specimens, which yield distinct XRD data. These samples were analyzed using high resolution transmission electron microscopy (HRTEM) and the stacking error distribution was directly determined. The HRTEM results compare well to those deduced by matching the XRD data with simulated spectra, confirming the hypothesis that the XRD data is indicative not only of the presence and density of stacking errors, but also that it can yield information regarding their distribution. In addition, the stacking error population in both specimens is related to their synthesis conditions and it appears that it is similar to the relation developed by others to explain the formation of the corresponding polytypes.

1

I. Introduction

Experimental XRD data from nominally β-SiC (or 3C) specimens, often contain several additional features, including occurrence of extra peaks, peak broadening, enhanced background around the 35.7° (0.252 nm) peak, peak shifts and reduced peak heights, which are due to the presence of stacking errors. In earlier work[1,2], we described computer simulations based on a selectively activated Ising model, which can generate β-SiC stacking sequences with different spatial distribution of stacking errors[§] and calculate their diffraction patterns[2]. Using these simulations, a direct correlation between the spatial distribution of stacking errors and the magnitude of the diffraction features was demonstrated. Variations in the magnitude of these features in XRD patterns, as have been observed among β-SiC particulates synthesized under different conditions, can be attributed to differences in the spatial distribution of stacking errors. In an earlier paper, differences between experimental diffraction patterns obtained from two different β-SiC specimens were briefly illustrated. As discussed in this paper, the simulation results have since been confirmed with high resolution transmission electron microscopy observations of stacking errors in specimens taken from the same lots of particulates.

Polytypic transformations play a crucial role in the microstructural development of SiC ceramics, and controlling these transformations is key to achieving desired mechanical properties[3-5]. In particular, detailed TEM studies of these polytypic transformations have shown that the propensity for these transformations as well as the resultant polytype during sintering are dictated to a large extent by the spatial distribution of stacking errors in the starting powder[5-7]. Although TEM techniques have been instrumental in establishing this correlation, determining the average distribution of

---

[§] As described in our previous papers, a *stacking error* is an error in the regular cubic stacking sequence. Thus a single stacking error generates a twin fault, stacking errors in adjacent layers generate an intrinsic fault, stacking errors separated by an error-free layer generate an extrinsic fault, and stacking errors separated by two or more error-free layers generate microtwins.

stacking errors in the starting powders or monitoring changes in error distribution/polytypic transformations during sintering can be tedious, if not practically impossible, using TEM. Carduner *et al.*[8] recently reported correlation between stacking disorder and features in NMR spectra, and demonstrated the applicability of NMR techniques in gaining qualitative information about stacking disorder in SiC. The present paper illustrates the utility of our simulation model in gaining qualitative information about the spatial distribution of stacking errors from XRD patterns, which can complement information obtained from NMR. Both these techniques can provide information about stacking errors quickly, and can form important tools in understanding polytypic transformations and microstructural evolution in SiC ceramics.

II. Experimental

(1) Materials Used

Two β-SiC specimens, which exhibited distinct diffraction patterns, were analyzed in this study. One of the specimens was a commercial β-SiC powder (Ibiden Co.), which is synthesized by the carbothermal reduction of silica by a carbon-containing vapor at temperatures typically less than 1500 °C. The Ibiden powder consists of equiaxed, nominally sub-micron grains with an average particle size of 0.3 μm and a narrow particle size distribution. The other β-SiC specimen was a reaction-formed SiC (RFSC), which is synthesized by a reactive melt infiltration technique. A distinctive feature of the RFSC process from other melt infiltration techniques is that no SiC filler is used in the preform, and as a consequence, all the SiC is formed *in situ* during infiltration. Also under the conditions used in the RFSC process, the SiC grains have had the opportunity to undergo appreciable coarsening by dissolution and reprecipitation so that the grains are well faceted crystals. In addition, although the temperatures at which infiltration is carried out is 1400-1500 °C, local temperatures can exceed 2000 °C during

3

SiC formation due to the exothermic reaction between Si and C. This implies that a part of the SiC grain growth occurs at temperatures significantly higher than the nominal infiltration temperatures. Details of the RFSC process, including a description of the mechanism of microstructural evolution are reported elsewhere[9-11].

(2) Techniques

All the experimental XRD data were obtained from powder samples on an X-ray diffractometer (Philips) using Cu-Kα radiation with a Ni filter. The data were acquired in the step-scan mode using 0.02° steps with 5 s time interval at each step in all the cases. The Ibiden powders were analyzed in their as-supplied condition. The RFSC specimens, which were obtained in the form of cylindrical shapes (approximately 15 mm, both in diameter and height), were crushed to powder using a mortar and pestle for XRD analysis. The RFSC specimens contained up to 15 vol.% residual silicon, but since the Si diffraction peaks do not interfere with those from SiC, no effort was made to remove the silicon from these samples prior to XRD analysis.

The spatial distribution of stacking errors in the two specimens, based on features observed in the experimental XRD data, was derived using iterative comparison of computer simulations to experimental XRD data. The simulation model, details of which are described in the earlier paper[2], generates stacking sequences with two distinct domains: an *error-free-domain* and an *Ising-domain*. By default, layers with cubic stacking, *i.e.*, sequences in the error-free domain, are generated, unless a "switch" to the Ising domain is specified. P_f, P_r, and U are the three simulation variables in the stacking algorithm that are used to specify the frequency of switching from the error-free to the Ising-domain, the volume fraction of layers generated within the Ising-domain, and the density of stacking errors within the Ising-domain, respectively. It was demonstrated in the earlier paper[2] that varying the values of the three variables could generate a wide

4

variety of spatial distributions of stacking errors. Each of these variables has a distinct influence on the spatial distribution of stacking errors, which in turn correlates with the resultant diffraction pattern.

Specimens for HRTEM studies were prepared using conventional techniques. The Ibiden β-SiC powders could be observed directly without any further thinning. Powder particles were captured on a 200 mesh size TEM copper grid by dipping the grid into a 5 vol.% particulate methanol-based suspension. In the case of RFSC specimens, slices of ~0.5 mm thickness were first cut from the as-received cylindrical specimens. Disks of 3 mm diameter were obtained from these slices using an ultrasonic disc cutter, which were then polished using 3 and 1μm diamond pastes to approximately 100 μm thickness. These thin disks were mounted on a copper grid, dimpled to ~35 μm thickness at the center, and further thinned to electron transparency by Ar-ion milling. All the HRTEM micrographs were obtained (using a JEOL 4000EX microscope) by aligning the beam close to the (110) zone axis for cubic SiC, so that stacking sequences could be identified directly from the micrographs.

III. Results

(1) Experimental X-ray Diffraction

Figure 1 shows experimentally observed diffraction data for both the Ibiden powders and the RFSC specimen together with the theoretically calculated pattern for β-SiC (which assumes an unfaulted 3C structure for the material and peak broadening due to instrument only[†]). The experimentally obtained patterns differ significantly from the ideal. Since instrumental broadening effects have been incorporated in the calculated pattern, the excessive broadening (see Table 1) observed in the experimentally obtained

---

[†] The instrumental broadening was determined to be 0.125° by experimentally running a standard silicon sample under the same conditions as those employed for the SiC specimens.

5

patterns relative to that for the calculated pattern must be due to intrinsic characteristics of the material, such as particle size, stacking faults, dislocations or variations in the layer-spacing.

As illustrated in Figure 1, XRD data for the RFSC specimen reveal modest broadening of both peaks and a lower height for the 41.6° (d = 0.217 nm) peak when compared to the calculated pattern. Also, the pattern shows gradual enhancement in the background intensity around the 35.7° peak, but no additional peaks are visible. In contrast, the pattern from the Ibiden powder shows significant peak broadening in both peaks relative to that of the calculated patterns. The broadening is more pronounced for the 41.6° peak than for the 35.7° peak (Figure 1 and Table 1). The data for the Ibiden powder also show considerable enhancement in the background intensity around the 35.7° peak, including evidence of a small peak at 33.7° (0.266 nm) and a very diffuse peak centered around 38.3° (0.235 nm). In neither of the experimental patterns, are shifts in the peak positions observed.

Earlier results using computer simulations have shown that all of the aforementioned additional features in the XRD data can be due to stacking faults in the β-SiC materials[1,2]. In addition, based on the correlation developed in the simulation between the relative magnitude of these features and the spatial distribution of stacking errors, several qualitative inferences about the distribution of stacking errors in these specimens can be made. In both experimental patterns, the enhancement in the background intensity around the 35.7° peak is not accompanied by a proportional broadening or shift in the 41.6° peak, which based on our prior results and those of others, indicates that the distribution of stacking errors is bimodal, although to different extents in the RFSC and Ibiden powders. The high background intensity around the peak at 35.7° in the Ibiden powders suggests an overall higher density of errors relative to that in the RFSC specimens. Furthermore, as discussed in our earlier paper[2], the additional

peaks at 33.7° and 38.3° and the resulting steep increase in the background intensity beginning at 33.7° for the Ibiden powders suggest that the error clusters contain a significant fraction of 1-layer and 2-layer microtwins (equivalent to intrinsic and extrinsic faults). The data from the RFSC specimen, on the other hand, show a smooth increase in intensity of this shoulder, which suggest that the error clusters in this specimen contain mostly 3-layer or wider microtwins.

(2) Stacking Error Distribution in the RFSC Specimens

By examining the simulated patterns in Part I, and performing additional iterations by trial and error, it is seen that features in the experimental diffraction pattern from the RFSC specimens can be reproduced in the simulations by specifying $P_f = 0.02$, $P_r = 0.95$ and $U = 10$ and $\Gamma_{sim} = 0.15°$ (Figure 2)[¶]. As shown in Table 1, the FWHM of both peaks in the experimental data matches very well with those from the simulations. The prescribed FWHM, $\Gamma_{sim} = 0.15°$, for the RFSC data is slightly higher than the expected 0.125° when only instrumental broadening is assumed, which suggest a modest contribution (of 0.025°) to peak broadening from factors other than instrumental broadening and stacking errors.

Figure 3 shows two HRTEM micrographs from adjacent regions within the same RFSC grain. The grain clearly shows the presence of error clusters together with error-free regions, *i.e.*, a bimodal distribution of stacking errors, in complete agreement with the simulation results. Additionally, within the error clusters, microtwins are usually 3 or more layers wide. In most grains, the stacking errors were usually confined to only one set of (111) planes, consistent with the assumption used in the simulations. However,

---

[¶] Γ_{sim} represents the full width at half-maximum (FWHM) specified in the simulations. It accounts for all factors contributing to peak broadening other than that due to stacking errors (see Section III(3) for a more descriptive explanation).

grains containing stacking errors in multiple planes, similar to that observed in the Ibiden powders (discussed in the next section), were also occasionally observed.

Furthermore, the stacking sequence in the RFSC grain determined from the HRTEM micrographs in Fig. 3, was used as the input stacking sequence in the simulations. The calculated diffraction pattern for this supercell (Figure 4) shows that it contains all the features observed in the experimental pattern, thus verifying that the stacking disorder observed by HRTEM is representative of the specimen. In addition, spatial distribution of stacking errors observed in the HRTEM micrographs and that obtained from the simulations are shown in Figure 5. In this figure, the histogram of the error distribution obtained from the HRTEM micrographs is based on a total of ~2500 layers from three different grains, while that from the simulated sequence (*i.e.*, the error distribution obtained for $P_f = 0.02$, $P_r = 0.95$ and $U = 10$) is based on a total of ~15000 layers (15 supercells). Even though the number of layers observed by HRTEM is limited, the simulation results are consistent with the HRTEM observations.

(3) Stacking Error Distribution in the Ibiden Powders

By using a similar approach as that for the RFSC specimens, it was found that a diffraction pattern generated using $P_f = 0.05$, $P_r = 0.95$, $U = 20.00$, and $\Gamma_{sim} = 0.25°$, could reproduce all the diffraction features observed in the Ibiden powders, as shown in Figure 6. The specified FWHM, Γ_{sim}, is significantly higher than the expected value of $0.125°$ due to instrumental broadening. The reason for this large discrepancy, although not apparent from the XRD results, becomes obvious from the HRTEM observations of these powders.

Figure 7 shows HRTEM micrographs from two different SiC grains in the Ibiden powder imaged along the cubic (110) zone axis. Consistent with the XRD and simulation results, the micrographs reveal the presence of several intrinsic and extrinsic faults

8

together with regions that are relatively error-free. In addition, the micrographs show that the stacking errors are not confined to a single set of (111) planes within the grain, which contradicts one of the assumptions in the simulations. Detailed observations of the stacking error configuration reveals, however, that the individual grains can be sub-divided into domains within which the stacking errors are predominantly confined to a single set of planes. Diffraction from such grains would be equivalent to that from crystallites with only single plane stacking errors, but with an effective particle size corresponding to the characteristic dimension of individual domains within each grain. Since the effective size of the particles is reduced, the experimental XRD pattern is expected to exhibit particle size peak broadening in addition to that due to stacking errors and instrument. This is mathematically verified and confirmed further as follows.

The total FWHM, Γ_t, observed in the experimental patterns can be expressed as

$$\Gamma_t^2 = \Gamma_{std}^2 + \Gamma_{se}^2 + \Gamma_{ps}^2 + \Gamma_{ls}^2 \tag{1}$$

where Γ_{std}, Γ_{se}, Γ_{ps}, and Γ_{ls} represent the contribution to peak broadening due to the instrument, stacking errors, particle size and variations in layer spacing. The FWHM specified in the simulations, Γ_{sim}, accounts for all factors contributing to peak broadening except that due to stacking errors, *i.e.*, it represents the sum of instrumental, particle size and layer spacing effects. Of these, the contribution to broadening due to variations in the layer spacing, Γ_{ls}, is presumed insignificant, and is ignored. Thus

$$\Gamma_{sim}^2 \approx \Gamma_{std}^2 + \Gamma_{ps}^2 \tag{2}$$

Since $\Gamma_{sim} = 0.25°$, and $\Gamma_{std} = 0.125°$, from equation (2),

$$\Gamma_{ps} \approx 0.23° \text{ or } 4.0 \text{ X } 10^{-3} \text{ rad.}$$

Using the following relation[12] for the effective particle size, t,

9

$$t = \frac{0.9\lambda}{\Gamma_{ps} \cos\theta} \qquad\qquad (3)$$

we obtain $t \approx 40$ nm, which is consistent with the size of the individual domains observed in the HRTEM micrographs.

(4) Spatial Distribution of Stacking Errors

Figure 8 shows the frequency distribution of stacking errors in the simulated sequences that reproduced the experimental patterns in both the RFSC and the Ibiden powders. In both cases, the histograms confirm that the distribution of stacking errors is bimodal. In these histograms, the ratio of the magnitude of the first peak to that of the second peak is a measure of the relative volume fraction of error-free regions, while the position of the second peak is a measure of the density of errors within the error-clusters. Clearly, the RFSCs show both a lower volume fraction of error-clusters and a lower density of stacking errors within the error-clusters. The histogram of the frequency distribution of microtwin widths in the simulated runs (Figure 9) provides further information about the spatial distribution of errors primarily within the clusters. Consistent with the HRTEM results, the simulated sequence for the Ibiden powder shows a high frequency of intrinsic (1-layer microtwin) and extrinsic (2-layer microtwin) faults while that for the RFSC specimen contains mostly wider band microtwins.

It is also of interest to examine the spatial distribution of different microtwins within the clusters, since repeated occurrence of microtwins of the same widths represent lamellae of specific α-polytypes (for example, 4 successive 2-layer microtwins in the cubic sequence are equivalent to two unit cells of 4H). If we arbitrarily specify that lamellae which consist of at least two continuous unit cells of an α-polytype constitute a region of the corresponding α-polytype, it is seen that the ratio between the different α-polytypes (2H, 4H and 6H) is similar to that between the corresponding microtwins (1-layer, 2-layer and 3-layer, respectively) as shown in Figure 11. However, the total

volume fraction of such different α-polytype regions in the simulated sequences is considerably lower than those of the corresponding microtwins. Shinozaki and Kinsman experimentally observed a similar correspondence in CVD grown β-SiC specimens[7].

The occurrence of error-clusters or lamellae of faulted sequences is very common in β-SiC specimens, and is observed, although to varying extents, in β-SiC specimens synthesized by different methods. Shinozaki and Kinsman[7] observed that the clusters often corresponded to one of the α-polytypes, *i.e.*, the clusters contained a periodic distribution of stacking errors. In particular, based on HRTEM studies by Jepps and Page[13], 3C crystals undergoing transformation to 6H have been shown to contain lamellae of 6H during the initial stages of transformation. The presence of such α-lamellae, therefore, has been regarded as the precursors to a β→α transformation. Our HRTEM results show that not all fault clusters necessarily consist of periodically occurring stacking errors. However, whether or not an error cluster corresponds to an α-polytype can often be very ambiguous, since the so-called α-lamellae contain significant amounts of stacking errors with respect to the α-polytype, and are only a few unit cells in thickness. In any case, irrespective of the degree of order within the clusters, it is clear that the distribution of stacking errors is almost always bimodal.

The magnitude of the simulation variables in the two cases, also raise some interesting questions. In both specimens studied here, P_r is 0.95, which is suggestive of the strong tendency for forming error clusters. Both P_f and U, however, are relatively large for the Ibiden powders compared to those for the RFSC specimens, *i.e.*, the Ibiden powders exhibit a higher frequency of clusters as well as a higher density of stacking errors within the clusters. Since the Ibiden powders are synthesized at temperatures significantly lower than those used in the synthesis of the RFSCs, this might appear to be contrary to expectations. However, this correlation between synthesis conditions and the observed types of stacking errors are remarkably similar to those observed in the

11

formation of the corresponding polytypes[14,15] - the 2H polytype (which corresponds to intrinsic faults in 3C) is observed to form at lower temperatures(1400-1500 °C), while the 4H and 6H polytypes (which correspond to extrinsic and 3-layer microtwins in 3C) form only at higher temperatures (>1900°C).

Differences in the synthesis conditions for the two specimens can also explain the occurrence of stacking errors on multiple (111) planes in the Ibiden powders. Stacking errors could occur on multiple (111) planes when growth of SiC layers occurs on more than one set of (111) planes in the crystal, or when two or more crystallites, each of which has faults only on a single set of planes, coalesce during growth. In either case, stacking errors are confined to a parallel set of (111) planes within any region in the grain although different regions of the same grain can exhibit stacking errors on different sets of (111) planes, as observed in the Ibiden powders. The near absence of such grains in the RFSC specimens is attributed to the substantial recrystallization, which occurs during their synthesis[9-11] and would be expected to eliminate such energetically unfavorable configurations.

(5) Correlation between Diffraction Data and Stacking Error Distribution

The correlation between features in diffraction data and the underlying spatial distribution of stacking errors in β-SiC specimens parallels those of Carduner et al.[8], who reported similar correlation between features in ^{29}Si solid-state NMR spectra and the underlying stacking disorder in several commercial β-SiC specimens. Thus experimental XRD data, like the NMR spectra, contain information about error distribution, and the technique can be potentially used to gain qualitative information about distribution of stacking errors in β-SiC specimens. Although neither XRD nor NMR can provide a unique description of the stacking disorder as obtained from a direct technique like HRTEM, it is possible to establish correlation between the XRD, NMR and TEM results

and exploit the convenience of NMR and XRD techniques in extracting information about stacking disorder. In particular, these techniques offer the potential for rapid monitoring of changes in stacking error distribution, which can be very useful in gaining insight into the influence of spatial distribution and density of stacking errors on polytypic transformations and subsequent microstructural development during sintering. Moreover, TEM results are based, due to practical considerations, on information from only a few grains. Since XRD and NMR techniques scan a larger area of the specimen, information from these techniques about the stacking order can be used to ascertain whether or not the HRTEM results are representative of the observed specimen. Thus information obtained from NMR and XRD techniques can also complement the HRTEM results.

Furthermore, as pointed out in previous papers, determination of polytype content using conventional XRD methods, which equate experimentally observed XRD intensities with those calculated from the crystal structure of several polytypes, often give misleading results[1,2] in the case of SiC. This is primarily due to the influence of stacking errors on the relative intensities of XRD peaks. It is anticipated that incorporating these simulations into the analysis routines would allow more reliable results about the polytype content to be obtained from the XRD data.

VI. Conclusions

The HRTEM observations of the population of stacking errors confirm that computer simulations based on the selectively activated Ising model can successfully reproduce stacking sequences in different β-SiC specimens. Such simulations can be applied to experimental XRD patterns to gain insight into the spatial distribution of stacking errors, and offer the possibility of rapid monitoring of changes in the stacking error and polytype distribution in these materials. Conditions that result in the formation

13

of particular error types are substantially similar to those that favor the formation of the corresponding polytypes, thus corroborating the hypothesis that stacking errors and polytypism in SiC are intricately related.

Acknowledgments

References

1. V. V. Pujar and J. D. Cawley, "Effect of Stacking Faults on the X-ray Diffraction Profiles of β-SiC Powders," *J. Am. Ceram. Soc.*, **78**[3] 774-82 (1995).

2. V. V. Pujar and J. D. Cawley, "Computer Simulations of Diffraction Effects due to Stacking Faults in β-SiC, I. Simulation Results," *J. Am. Ceram. Soc.*, **80**[7] 1653-62 (1997).

3. S. Prochazka, "Abnormal Grain Growth in Polycrystalline SiC," *Proc. Third Inter. Conf. on Silicon Carbide, Miami, FL*, 394-402 (Sept. 1973).

4. N. P. Padture, "In Situ-Toughened Silicon Carbide," *J. Am. Ceram. Soc.*, **77**[2] 519-23 (1994).

5. A. H. Heuer, G. A. Fryburg, L. U. Ogbuji, T. E. Mitchell, and S. Shinozaki, "β–α Transformation in Polycrystalline SiC: I, Microstructural Aspects," *J. Am. Ceram. Soc.*, **61** [9-10] 406-12 (1978).

6. N. W. Jepps and T. F. Page, "Polytypic Transformations in Silicon Carbide," *Prog. Cryst. Growth Charact.*, **7**, 259-307 (1983).

7. S. S. Shinozaki and K. R. Kinsman, "Aspects of 'One Dimensional Disorder' in Silicon Carbide," *Acta Metall.*, **26**, 769-776 (1978).

8. K. R. Carduner, S. S. Shinozaki, M. J. Rokosz, C. R. Peters, and T. J. Whalen, "Characterization of β-Silicon Carbide by Silicon-29 Solid State NMR, Transmission Electron Microscopy, and Powder X-ray Diffraction," *J. Am. Ceram. Soc.*, **73**[8] 2281-86 (1990).

9. V. V. Pujar, J. D. Cawley, and M. Singh, unpublished work.

10. Y.-M. Chiang, R. P. Messner, D. R. Behrendt, and C. D. Terwilliger, "Reaction-Formed Silicon Carbide," Mater. Sci. Eng., **A144**, 63-74 (1991).

11. M. Singh and D. R. Behrendt, "Microstructure and Mechanical Properties of Reaction-Formed Silicon Carbide (RFSC) Ceramics, Mater. Sci. Eng., **A187** [2] 183 (1994).

12. B. D. Cullity, "Elements of X-ray Diffraction," pp.284, Addison-Wesley Publishing Co., Inc. (1978).

13. N. W. Jepps and T. F. Page, "Intermediate Transformation Structures in Silicon Carbide," *J. Microsc.*, **119,** Pt. 1, 177-188 (1980).

14. R. F. Adamsky and K. M. Merz, "Synthesis and Crystallography of the Wurtzite form of Silicon Carbide," *Z. Krist.*, **111**, 350-361 (1959).

15. L. S. Ramsdell and J. A. Kohn. "Developments in Silicon Carbide Research," *Acta. Crstallogr.*, **5**, 215-24 (1952).

Figures

Figure 1.   X-ray diffraction data in the 30-45° 2θ range from reaction-formed β-SiC and Ibiden β-SiC powder. The calculated pattern for the 3C polytype is also included in the figure for comparison. Experimental diffraction data from both specimens differ significantly, but distinctly, from the calculated pattern.

Figure 2.   X-ray diffraction data for the RFSC specimen superimposed with a simulated pattern that closely matches the experimental data. The simulated pattern was obtained using $P_f = 0.015$, $P_r = 0.975$, $U = 5.00$ and $\Gamma_{sim} = 0.15°$.

Figure 3.   HRTEM micrographs, (a) and (b), of RFSC specimens from adjacent regions along a cubic (110) zone axis showing the presence of fault clusters together with large fault-free-regions within the same grain. Also, stacking errors are confined to a single set of (111) planes.

Figure 4.   X-ray diffraction data for the RFSC specimen superimposed with a calculated pattern. The calculated pattern was obtained by specifying the stacking sequence observed in the HRTEM micrographs.

Figure 5.   Density frequency plots obtained from the HRTEM micrographs and simulations for the RFSC specimens.

Figure 6.   X-ray diffraction data for the Ibiden powder superimposed with the simulated pattern. The simulated pattern was obtained using $P_f = 0.05$, $P_r = 0.96$, $U = 20.00$ and $\Gamma_{sim} = 0.25°$.

Figure 7.   HRTEM micrographs of two different Ibiden β-SiC grains, (a) and (b), respectively, along a cubic (110) zone axis. In both cases, grains exhibit stacking errors along multiple (111) planes, but each grain can be further subdivided into domains in which errors are confined to a single plane.

Figure 8.   Density frequency plots in the simulated sequences whose diffraction data matched those from the RFSC and Ibiden specimens.

Figure 9.   Width frequency plots in simulated sequences whose diffraction data matched those from the RFSC and Ibiden specimens.

Figure 10.   Histogram of the volume fraction of different polytypic lamellae in the Ibiden powder and the RFSC specimen.

## Table 1. FWHM of peaks in experimental and simulated data

| Material/Simulation Parameters	FWHM (in °)	
	d = 0.252 nm	d= 0.217 nm
1. Unfaulted 3C (simulated)	0.125	0.125
2. β-SiC Ibiden Powder Specimen		
Experimental data	0.31	0.52
Simulated (P_f = 0.05, P_r = 0.95, U = 20.0, Γ_{sim} = 0.125)	0.17	0.47
Simulated (P_f = 0.05, P_r = 0.95, U = 20.0, Γ_{sim} = 0.250)	0.32	0.54
3. RFSC specimen		
Experimental data	0.21	0.25
Simulated (P_f = 0.05, P_r = 0.95, U = 20.0, Γ_{sim} = 0.15)	0.20	0.25
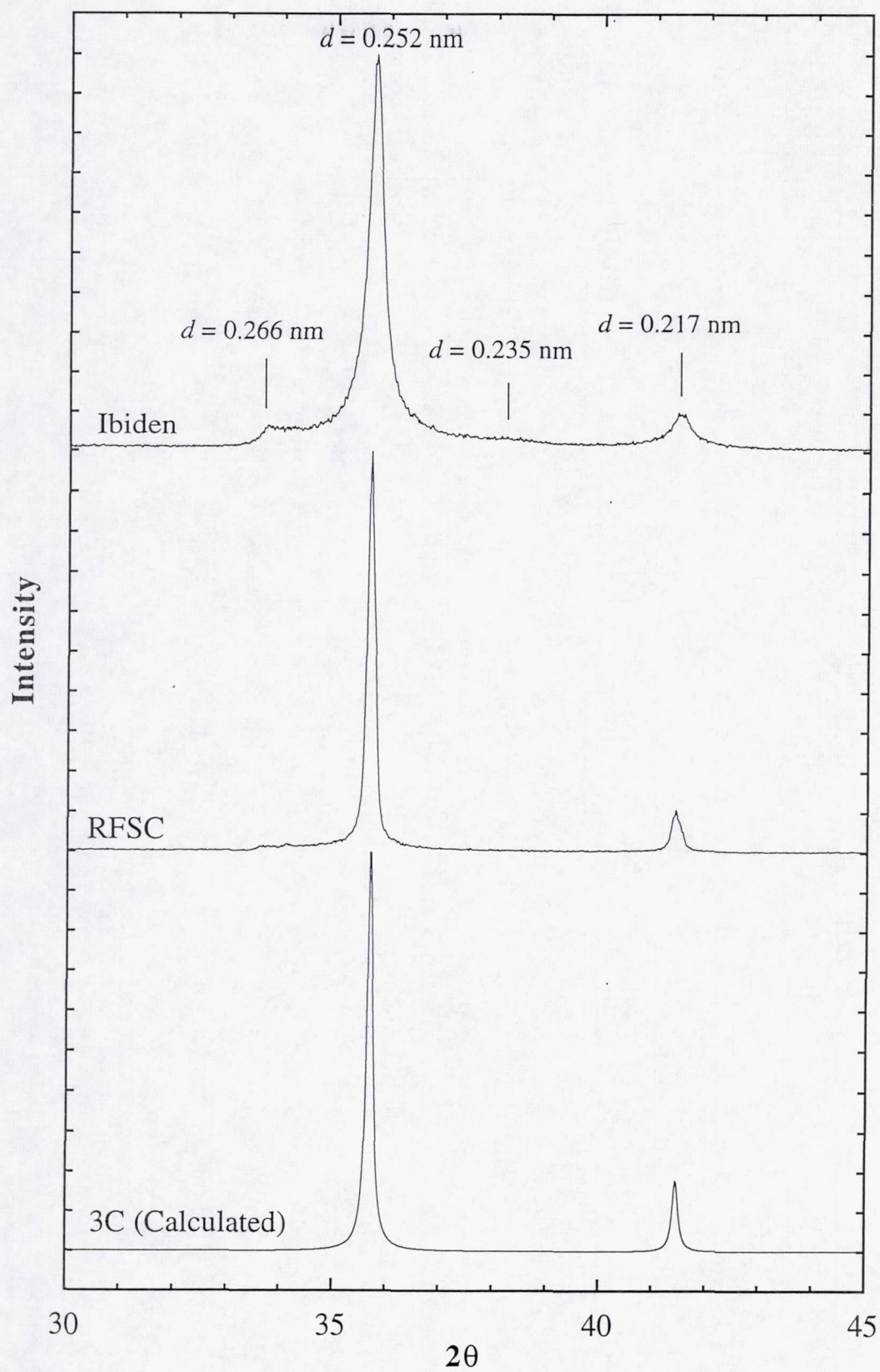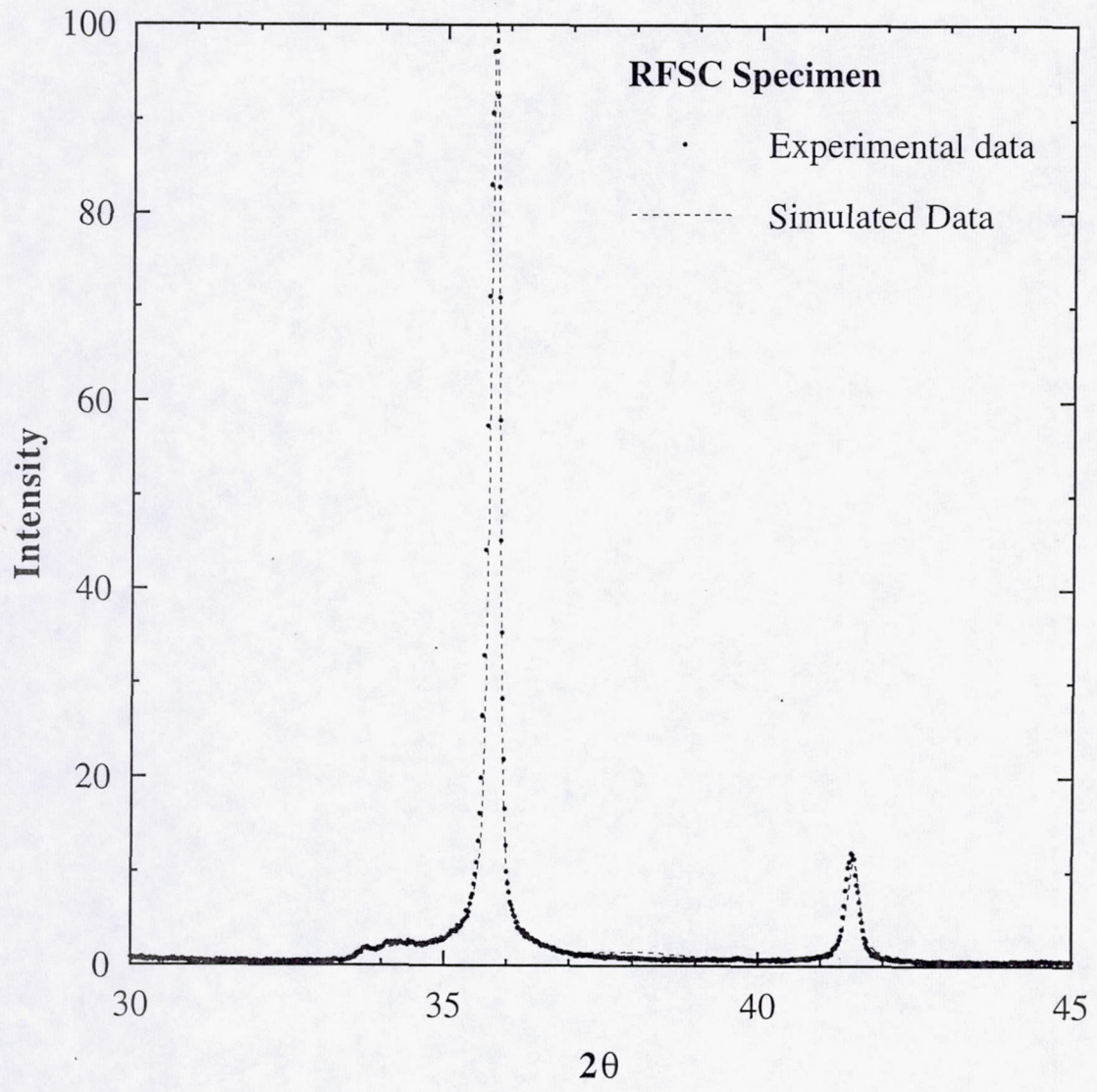
$d = 0.252$ nm

$d = 0.266$ nm

$d = 0.235$ nm

$d = 0.217$ nm

Ibiden

RFSC

3C (Calculated)

Intensity

2θ

30   35   40   45

Pujar and Cawley
Figure 1

RFSC Specimen

• Experimental data

------- Simulated Data

Pujar and Cawley
Figure 2

a

5 nm

Pujar and Cawley
Fig. 3(a)

b

5 nm

Pujar and Cawley
Fig. 3(b)

RFSC Specimen

· Experimental XRD data
------- Calculated Pattern
(from HRTEM sequence)

Pujar and Cawley
Figure 4

Reaction-Formed SiC

Simulations

HRTEM Observations

Faults/Layer

Pujar and Cawley
Figure 5

Ibiden Powder

· Experimental data

------ Simulated data

Intensity

2θ

a

5 nm

Pujar and Cawley
Fig 7(a)

b

5 nm

Pujar and Cawley
Fig 7(b)

Simulation data

Ibiden Powder

RFSC

Density Frequency

Stacking error   density (errors/layer)
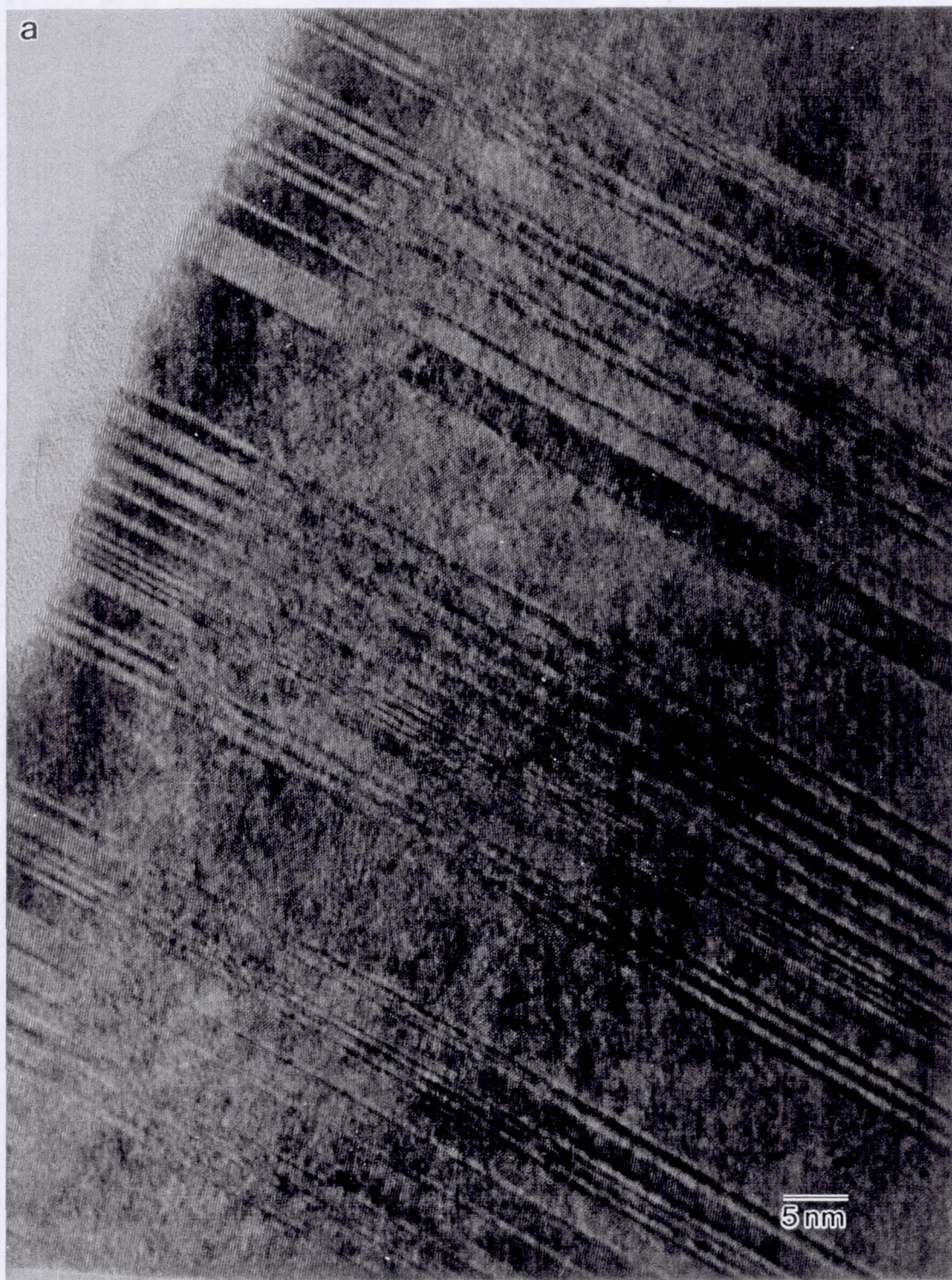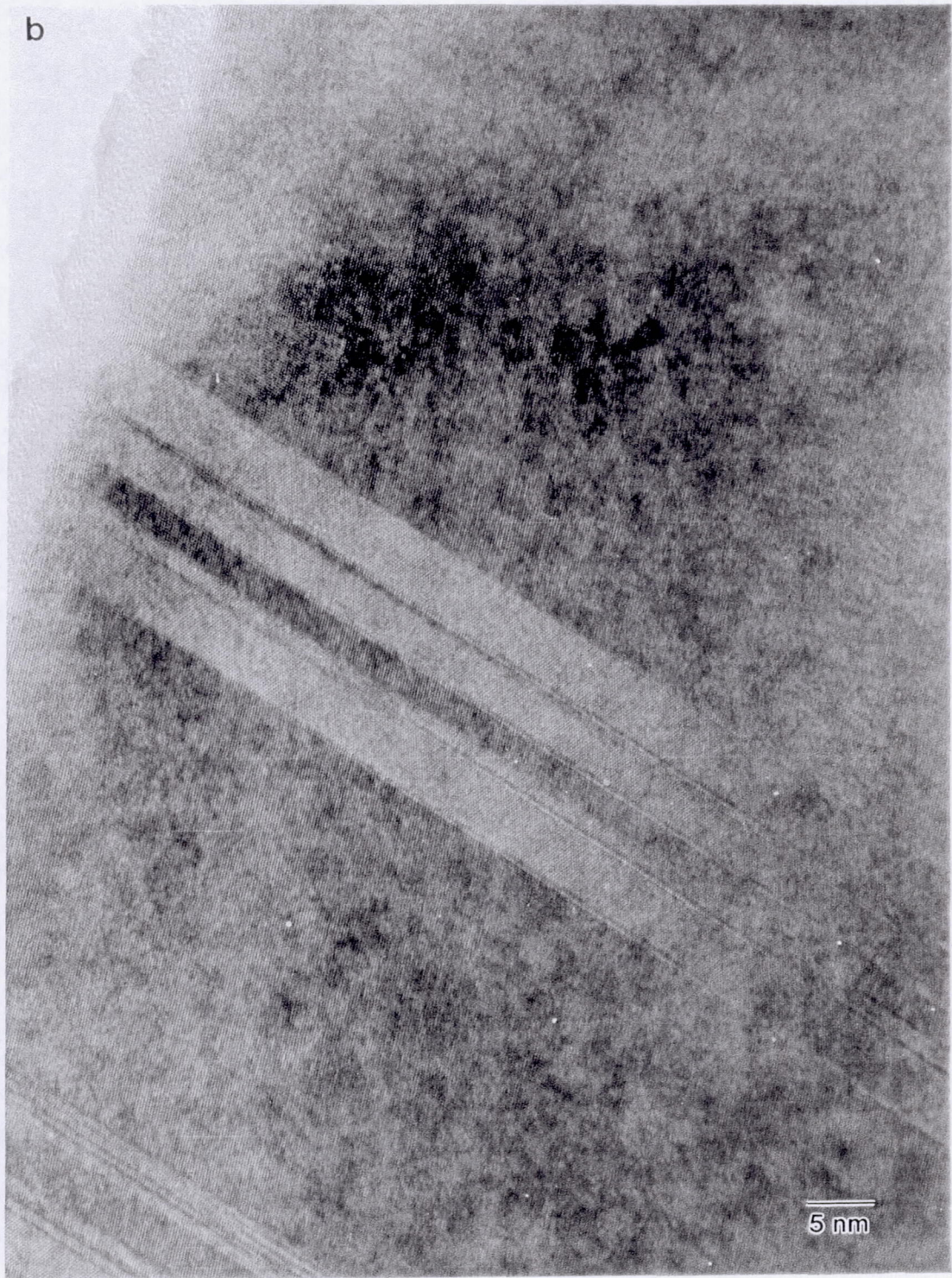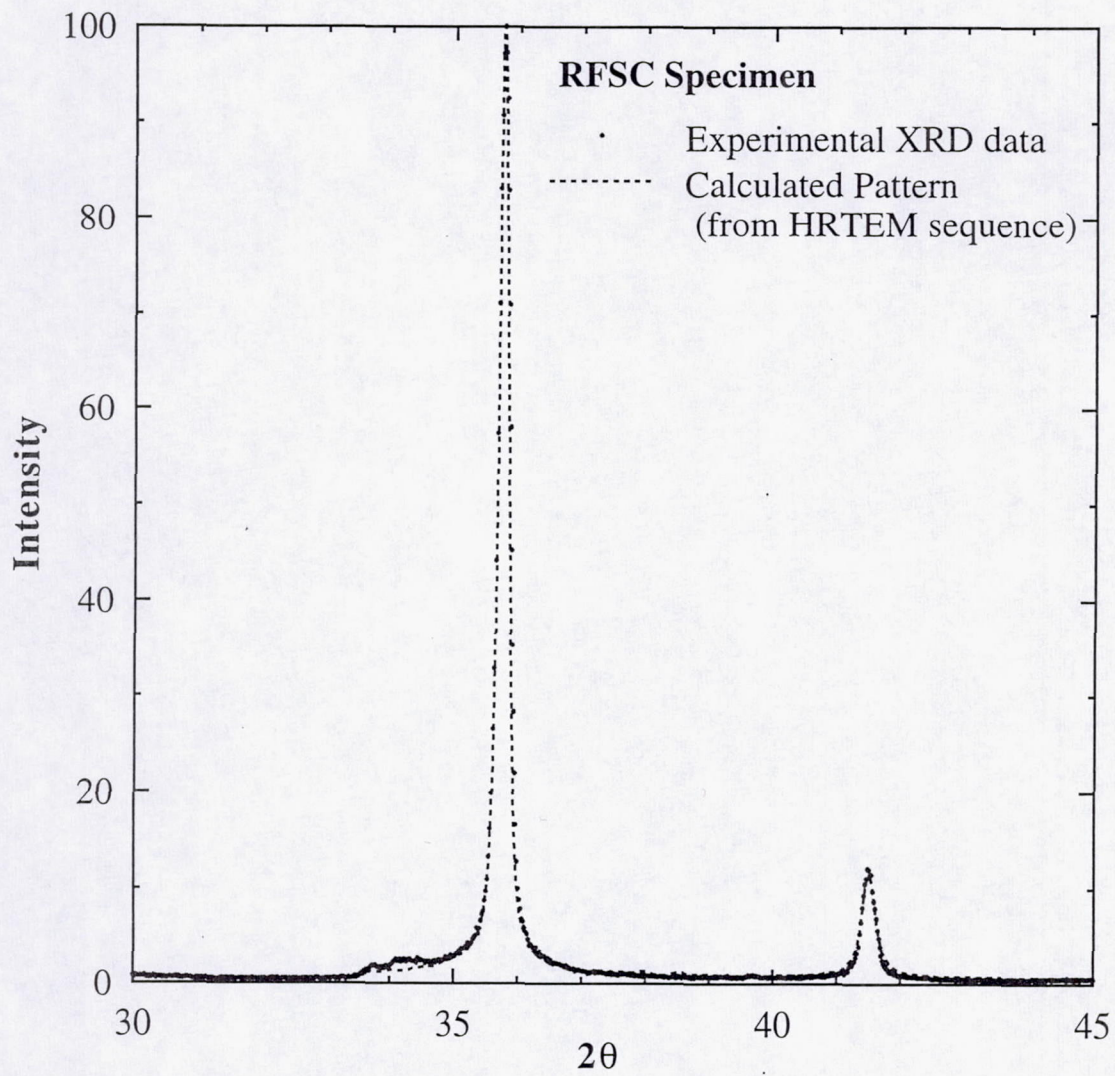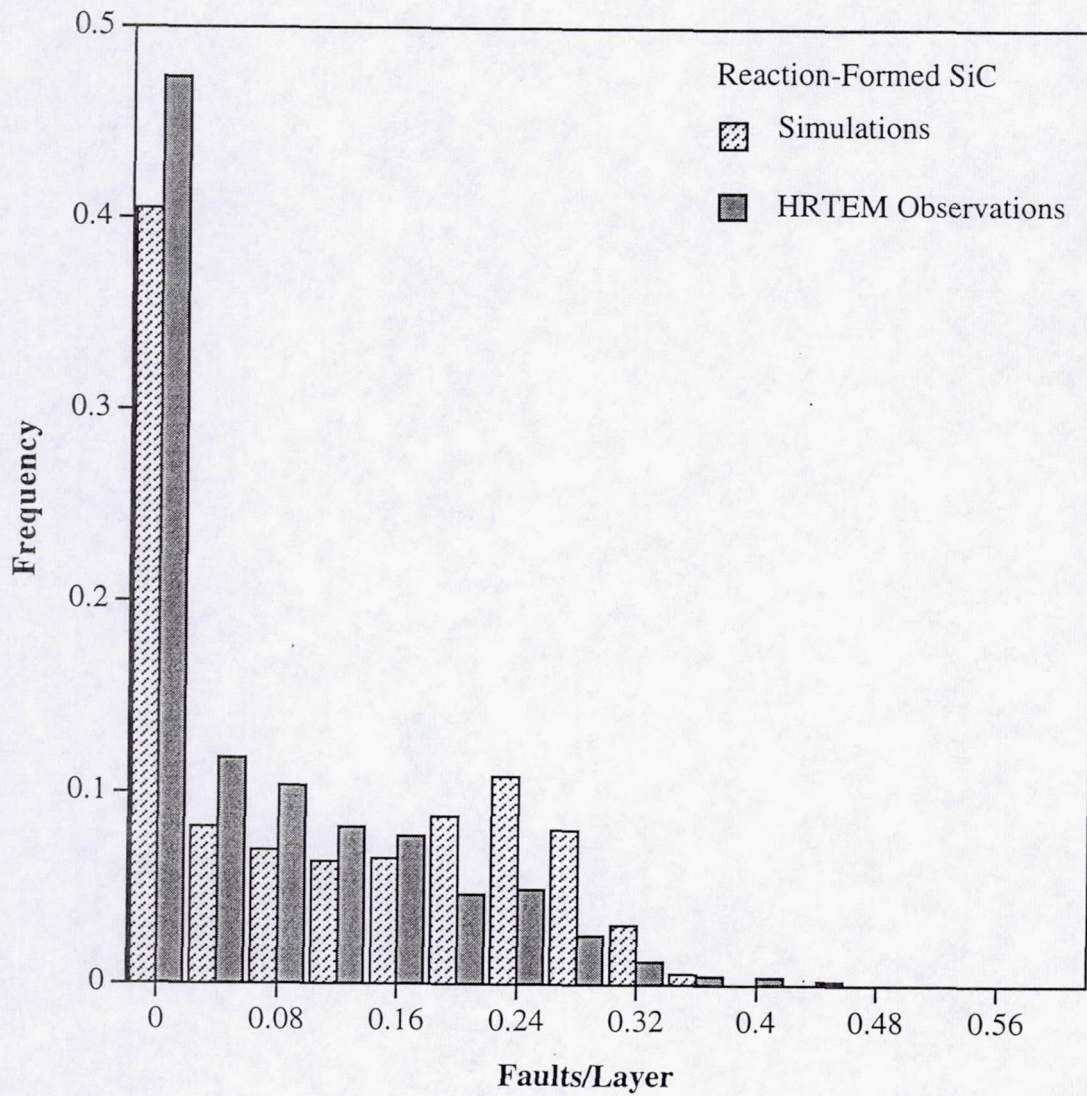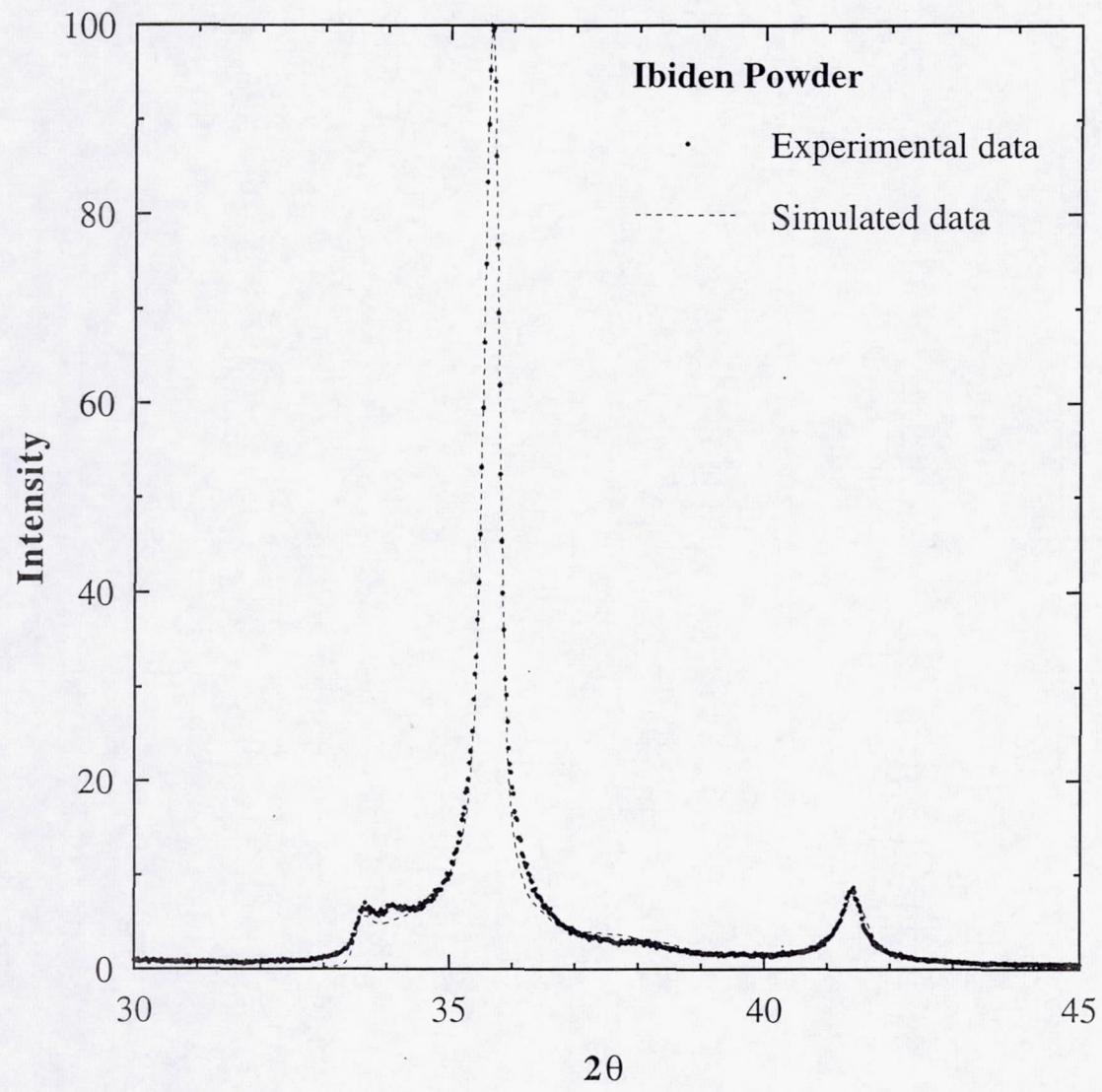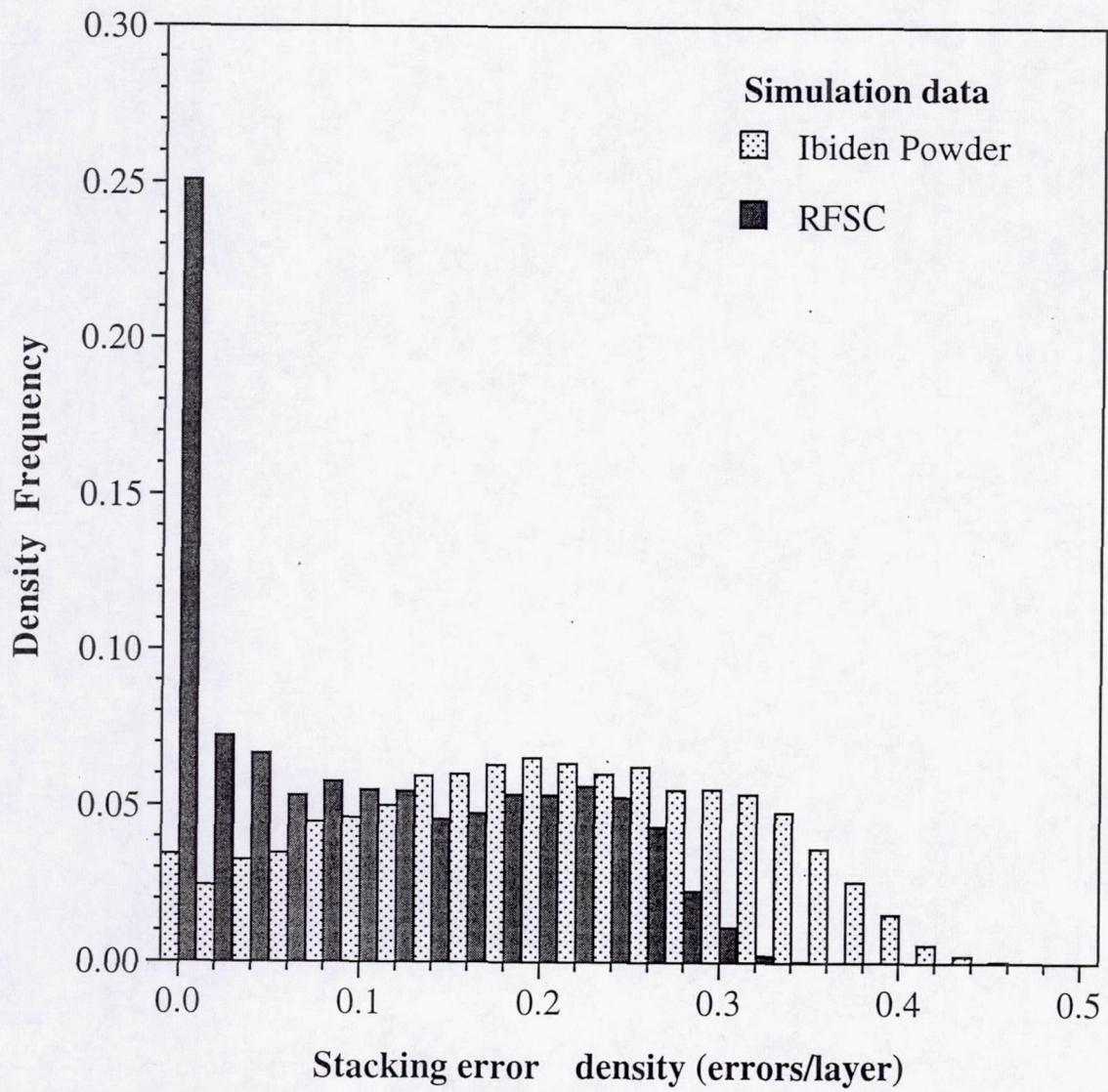
Pujar and Cawley
Figure 8

Pujar and Cawley
Figure 10